

Reactive compatibilization of harakeke fiber-reinforced poly(lactic) acid/polybutylene succinate blend

John O. Akindoyo¹  | Kim Pickering¹ | Mohammad Dalour Beg¹ | Michael Mucalo²

¹School of Engineering, University of Waikato, Hamilton, New Zealand

²School of Science, University of Waikato, Hamilton, New Zealand

Correspondence

John O. Akindoyo, School of Engineering, University of Waikato, Hamilton, New Zealand.
Email: blessedbode@gmail.com

Funding information

Ministry of Business, Innovation and Employment, Grant/Award Number: UOWX2004; University of Waikato, Grant/Award Number: Research & Enterprise Award (108023)

Abstract

Different blends of poly(lactic acid) (PLA) and polybutylene succinate (PBS), and their harakeke fiber-reinforced composites were studied. Scanning electron microscopy showed that the PLA and PBS are incompatible and poorly miscible. Tensile strength and tensile modulus of the blends were found to reduce as the amount of PBS increased. Reinforcement alone was not able to significantly improve the mechanical performance of the blend, which is lower than that of neat PLA. Therefore, simultaneous reinforcement and reactive compatibilization were performed using harakeke fiber, and dicumyl peroxide as reinforcement and compatibilizer, respectively. This produced about 201% increase in the crystallinity of PLA. Compared with the PLA/PBS blend, the dual effect approach increased the tensile strength and tensile modulus by 31% and 148%, respectively. Likewise, dynamic mechanical analysis showed that the thermomechanical properties of the composite greatly improved.

KEYWORDS

composites, mechanical properties, thermal properties, thermogravimetric analysis (TGA), thermoplastics

1 | INTRODUCTION

The rising environmental concerns associated with petroleum derived materials, and the growing awareness of the need to protect the environment have triggered an increased interest in environmentally friendly materials. As such, the past few decades have been graced with increasing efforts on the development of materials that can help to reduce global dependence on petroleum-based products.^{1–3} At the forefront of this drive are materials developed from renewable, biobased, or biodegradable polymer-based composites.^{4–6} This is partly due to the versatility of polymers, and their

property tunability for desired applications.⁷ In the last decade, there has been a continuous increase in the production of biopolymers, with a forecast estimating the global production of biopolymers to hit 2.43 million tons in 2024.^{4,8}

In particular, the rate of market growth of poly(lactic acid) (PLA) is higher than its contemporaries because of its properties, such as high mechanical strength, sufficient biodegradability or compostability, excellent biocompatibility, good processability, and large-scale availability at a competitive price.^{9–11} In addition, the production of PLA is reported to consume lesser energy (about 25%–55%) and generate lower CO₂ emissions than

This is an open access article under the terms of the [Creative Commons Attribution](https://creativecommons.org/licenses/by/4.0/) License, which permits use, distribution and reproduction in any medium, provided the original work is properly cited.

© 2024 The Author(s). *Journal of Applied Polymer Science* published by Wiley Periodicals LLC.

conventional petroleum-based plastics.^{12,13} Therefore, the use of PLA has become increasingly acceptable in different sectors including building and construction, biomedicine, food packaging, industrial parts, and in the automobile industry.^{14,15} However, to extend the applications of PLA in structural and engineering products, there is need to address its inherent brittleness, and small elongation at break.^{1,4,16}

One effective approach to reduce the brittleness and increase the elongation at break of PLA is to blend it with other rubbery elastomers or plastics.^{17,18} Blends of PLA with different plastics like polyethylene,¹⁹ polycaprolactone,²⁰ poly(butylene-adipate-co-terephthalate) (PBAT),²¹ and polybutylene succinate (PBS)²² have been investigated. Among these, PBS has the lowest environmental impact,²³ and it also has good processability like PLA. Hence, efforts have been made to improve the elongation at break of PLA by adding different composition ratios of PBS.²⁴ However, PLA and PBS are only partially miscible.¹⁶ This often results in decreased tensile strength (TS) and modulus as PBS content increased in PLA/PBS blends.^{25,26} In one study, a blend of PLA and PBS was reported to exhibit an elongation at break of 340% when the PBS content is 30 wt.%. However, this resulted in undesirable decreases in the TS and modulus of the blend.²⁷

Based on this, reactive processing is seen as an effective method for improving the miscibility of PLA and its blends. As such, different coupling agents have been used to improve the miscibility of PLA blends. For example, glycidyl methacrylate (GMA) was used by Zhang et al. to process PLA/PBAT blends.²⁸ This helped to improve the interfacial adhesion between PLA and PBAT and resulted in increased mechanical performance. Likewise, another study reports the reactive processing of PLA, polycarbonate (PC), and PBAT ternary blends in the presence of dicumyl peroxide (DCP) as processing aid.²⁹ In the case of PLA/PBS blends, different processing aids have been used. Supthanyakul et al. used random poly(butylene succinate-co-lactic acid) (rPBSL) to facilitate compatibility and clarity in PLA/PBS blends,²⁶ while Fortunati et al. prepared PLA/PBS films using acetyl tributyl citrate (ATBC) and isosorbide diester (ISE) as processing aids.²⁵ In addition, other agents such as lysine tri-isocyanate,³⁰ twice-functionalized organoclay (TFC),³¹ and DCP³² have been explored. Reports showed that the use of processing aids can help to improve miscibility and compatibility in the blends, thereby improving the elongation at break of PLA. However, there are still concerns about the decrease in strength and modulus of PLA as the amount of rubbery component increases.

Literature has also shown that the use of reinforcing fillers can help to improve the mechanical performance

of PLA and its blends. In particular, the use of biobased fillers is seen as an effective way to improve performance and reduce cost, while maintaining the environmental friendliness of the composite material. Hence, blends of PLA and PBS have been successfully prepared where biobased fillers such as kraft pulp, wood flour, bamboo powder, and microfibrillated cellulose (MFC) were used as reinforcement.^{33–35} However, to the best of the authors' knowledge, there are no reports that combine the reinforcement strategy with reactive compatibilization to produce reinforced PLA blends with improved mechanical performance. Therefore, in this article, harakeke fiber was used as a reinforcing filler to improve the TS and modulus of PLA/PBS blend. The choice of harakeke fiber is based on its confirmed capability to effectively reinforce PLA, as reported in previous studies.^{36,37} Then, DCP was used as a processing aid to improve the miscibility of PLA and PBS. The effect of PBS on the TS and modulus of PLA, the effect of the reinforcing filler on reinforced PLA/PBS blends, and the influence of reactive compatibilization are discussed.

2 | MATERIALS AND METHODS

2.1 | Materials

PLA was used as the polymer matrix in this study. This injection molding grade PLA biopolymer (Ingeo™ 3052D) from NatureWorks has a specific gravity of 1.24, while the melt flow rate (MFR) is 14 g/10 min (210°C, 2.16 kg). PBS (Bio-PBS FZ71) with a MFR of 22 g/10 min (190°C, 2.16 kg) and a density of 1.26 g/cm³ was supplied by PTT MCC Biochem Company Limited. DCP was purchased from Sigma-Aldrich and used for reactive compatibilization of PLA and PBS. Harakeke (New Zealand flax) fiber was used as the reinforcement and it was supplied by Templeton Flax Milling Heritage Trust, New Zealand. Bulk sodium hydroxide solid pellets were procured from Sigma-Aldrich and used to treat the harakeke fiber.

2.2 | Methods

2.2.1 | Fiber preparation, treatment, and analysis

The harakeke fibers obtained from the supplier were in bundles of about 1–1.5 m long. This material was first dried and chopped with a guillotine into pieces of about 2–3 cm. Weighed amounts of the chopped fiber were put in stainless steel canisters and a solution of 5 wt.% NaOH

TABLE 1 Sample codes and the amount (wt.%) of individual component in the different samples.

| Sample code | PLA (wt.%) | PBS (wt.%) | Fiber (wt.%) | DCP (wt.%) |
|---------------------------------|------------|------------|--------------|------------|
| PLA | 100 | - | - | - |
| PBS | - | 100 | - | - |
| PLA + 5% PBS | 95 | 5 | - | - |
| PLA + 10% PBS | 90 | 10 | - | - |
| PLA + 15% PBS | 85 | 15 | - | - |
| PLA + 20% PBS | 80 | 20 | - | - |
| PLA + 10% PBS + 30% fiber | 60 | 10 | 30 | - |
| PLA + 10% PBS + 30% fiber + DCP | 59.7 | 10 | 30 | 0.3 |

Abbreviations: DCP, dicumyl peroxide; PBS, polybutylene succinate; PLA, poly(lactic acid).

and 2 wt.% Na_2SO_3 was poured into the canister to obtain a fiber to solution ratio of 1:8. Then, fiber digestion was performed in a lab-scale pulp digester as described in literature.³⁸ The treated fiber was washed continuously with water until neutral pH was attained. Then, the fiber was dried in an oven at 80°C for 48 h and kept in sealed plastic bags until it was used for composite preparation.

Before the treated fiber was compounded with the matrix, it was examined under a BX53 Olympus optical microscope. Small amount of the fiber was placed on a glycerol droplet standing on a microscope glass slide. This was evenly spread on the glass slide, thereby facilitating the fiber dispersion. A second glass slide was placed on the dispersed fiber, and this was mounted on the sample holder of the microscope. After taking images of the fiber, an Olympus Stream image analysis software fitted with the microscope was used to measure the length and diameter of the images. About 100 measurements were taken, and it was found that the average length and diameter of the fiber were 3 mm and 12 μm , respectively.

2.2.2 | Production of blends and composites

Blends of PLA and PBS were prepared by varying the PBS content from 5% to 20 wt.%. The components were mixed and compounded using a TSE-16-TC twin-screw extruder at a screw speed of 100 rpm using a temperature profile in the range of 165–185°C. Composite material was prepared by compounding 30 wt.% harakeke fiber with a selected PLA/PBS blend. The wt.% fiber used was based on the preliminary study. In addition, a composite material containing PLA, PBS, harakeke fiber, and DCP was compounded in the extruder at the same conditions used for the blends and the composite without DCP. The amount (wt.%) of each component in the different category of composites prepared is presented in Table 1. Prior

to extrusion of the fiber containing composites, the treated fibers were processed in a blunt Sunbeam Multi-grinder to separate the fibers. Then the processed fibers were kept in a 105°C conventional oven until it was used. The PLA and PBS granules were dried to moisture content <0.1% in a vacuum oven set at 60°C for 2 h.

The extrudates were granulated with a Moretto GR knife mill plastic granulator to obtain <3 mm pellets. The granules were dried to a moisture content <0.1% by weight and was used to produce tensile test samples in a BOY 35A injection molding machine. The extrusion and injection parameters are summarized in Table 2. Digital images of raw and treated harakeke fiber and representative injection molded samples are presented in Figure 1.

2.2.3 | Scanning electron microscopy

Fractured surfaces of PLA, PBS, PLA/PBS blends, and the reinforced composites were examined on a Hitachi Regulus SU8230 field emission scanning electron microscope. It should be noted that PBS did not fracture during tensile testing. So, the scanning electron microscopy (SEM) image presented for PBS is from cryofracture samples. Double sided carbon tape was used to mount the dried samples on aluminum stubs, and the samples were then coated with a thin layer (5 nm) of platinum through sputtering in a Quorum Q150V sputtering equipment.

2.2.4 | Mechanical testing

In preparation for testing, injection molded tensile testing samples which were prepared according to EN ISO 527 specifications were first kept in a 23°C climate chamber for 48 h at 50% relative humidity. Tensile testing was then performed on a universal testing machine (Instron[®] 5982). The instrument is equipped with a 5 kN

TABLE 2 Extrusion and injection molding profiles for the preparation of PLA-PBS, PLA-PBS-fiber, and PLA-PBS-fiber-DCP composites.

| Extrusion parameter | Unit | PLA, blends, and composites | | Injection molding parameter | Unit | PLA, blends, and composites | |
|---------------------|-------|-----------------------------|-----------|-----------------------------|---------|-----------------------------|-----------|
| | | Value | PBS Value | | | Value | PBS Value |
| Feeding zone | (°C) | 165 | 60 | Feeding zone | (°C) | 150 | 100 |
| Zone 1, 2 | (°C) | 170 | 160 | Compression zone | (°C) | 165–185 | 130 |
| Zone 3, 4 | (°C) | 175 | 150 | Metering zone | (°C) | 190 | 140 |
| Zone 5, 6, 7, 8 | (°C) | 180 | 150 | Nozzle | (°C) | 185 | 150 |
| Zone 9 | (°C) | 180 | 140 | Mold | (°C) | 35 | 25 |
| Die | (°C) | 185 | 140 | Screw speed | (ccm/s) | 43.1 | 43.1 |
| Screw speed | (rpm) | 100 | 60 | Screw position | (mm) | 30 | 30 |
| | | | | Injection pressure | (bar) | 550–600 | 225 |
| | | | | Holding pressure | (bar) | 600 | 600 |
| | | | | Injection time | (s) | 0.5 | 0.72 |
| | | | | Cooling time | (s) | 30 | 40 |

Abbreviations: DCP, dicumyl peroxide; PBS, polybutylene succinate; PLA, poly(lactic acid).



FIGURE 1 Digital images of raw harakeke fiber, treated (digested) harakeke fiber, and representative images of injection molded samples. PBS, polybutylene succinate; PLA, poly(lactic acid). [Color figure can be viewed at wileyonlinelibrary.com]

load cell and was operated at a crosshead speed of 5 mm/min. Tensile strain on the samples during testing was measured with a 25 mm extensometer, which was fixed at the middle of the specimen. Five specimens were tested per composite category and the average values of the TS and tensile modulus (TM) were recorded.

2.2.5 | Thermogravimetric analysis

The thermal properties of the materials were performed in a Perkin Elmer STA 8000 thermal analyzer. About 10–20 mg of the samples were weighed and placed in a crucible. This was heated from 30 to 600°C at a rate of 10°C/

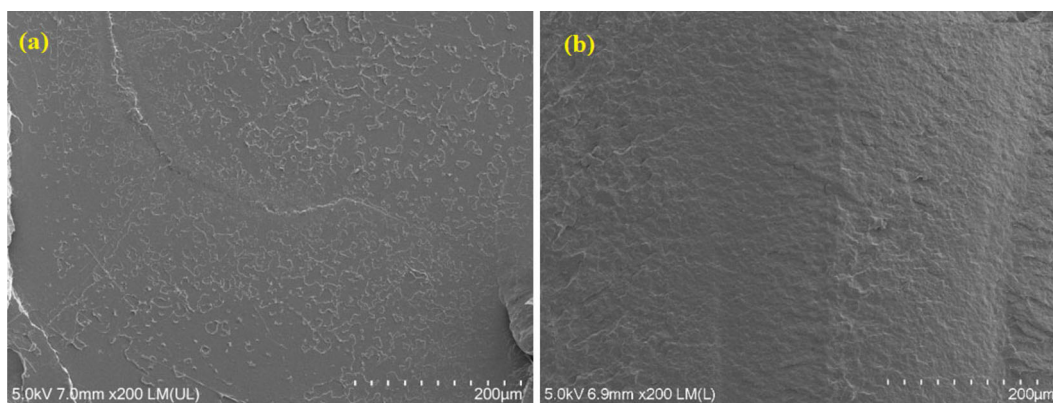


FIGURE 2 Scanning electron microscopy images of the fractured surface of (a) poly(lactic acid) after the tensile test, and (b) the cryofracture sample of polybutylene succinate. [Color figure can be viewed at wileyonlinelibrary.com]

min under an argon atmosphere, with a gas flow of 40 mL/min.

2.2.6 | Differential scanning calorimetric analysis

Differential scanning calorimetry analysis (DSC) of the materials was performed in a TA instrument (Netzsch DSC 3500 Sirius). The samples, with weights of 10–15 mg, were heated at a rate of 10°C/min from 20 to 200°C. Heating was performed under nitrogen gas flowing at 60 mL/min. The DSC thermogram obtained was used to determine the glass transition temperature (T_g), crystallization temperature (T_c), and melting temperature (T_m) of the samples. Furthermore, the crystallinity % (I_{DSC}) in the blend and composites was derived using the following equation:

$$\text{Crystallinity}\%(I_{DSC}) = \frac{\Delta H}{\Delta H_m W} \times 100\%,$$

where, ΔH is the enthalpy of fusion of the samples, ΔH_m is the enthalpy of fusion of a reference PLA with 100% crystallinity, and W is the mass fraction of the matrix. The crystallinity % (I_{DSC}) of the blend and composites was calculated by using 93.6 J/g as the enthalpy of fusion (ΔH_m) of reference PLA with 100% crystallinity.³⁶

2.2.7 | Dynamic mechanical analysis

The viscoelastic properties of the materials were assessed through dynamic mechanical analysis (DMA) using a Perkin Elmer DMA800 instrument. Samples with dimensions 30 mm × 5 mm × 1.5 mm were fitted in a single cantilever configuration and heated from 23 to 140°C at

2°C/min. The analysis was performed at a constant frequency of 1 Hz, while the displacement amplitude was 20 µm.

3 | RESULTS AND DISCUSSION

3.1 | Morphological properties

The SEM images of the fractured surface of PLA and PBS are shown in Figure 2. The image of PLA in Figure 2a reveals a smooth fracture which is typical of brittle materials like PLA. In contrast, the image of PBS in Figure 2b depicts an uneven fractured surface, associated with tough materials which supports that PBS is relatively tougher than PLA.

The SEM images of the fractured surface of PLA/PBS blends with different PBS content (5–20 wt.%) are presented in Figure 3. As seen in the image, the presence of dispersed voids created by the dispersed PBS in the continuous PLA matrix phase becomes increasingly noticeable as the PBS content increases. It is noteworthy that at the higher PBS contents, the domains of PBS were more conspicuous in the SEM images (as in Figure 3d). Similar observation has been reported by other researchers^{16,32} including spherical droplets of PBS conspicuously dispersed in the continuous PLA phase after blending. These domains indicate poor compatibility between PLA and PBS,^{16,39} and can influence the tensile performance of the blends as discussed in a subsequent section.

3.2 | Mechanical properties

The tensile properties of PLA, PBS, and PLA-PBS blends containing different wt.% (5–20 wt.%) PBS are presented in Figure 4. It is evident in Figure 4 that the

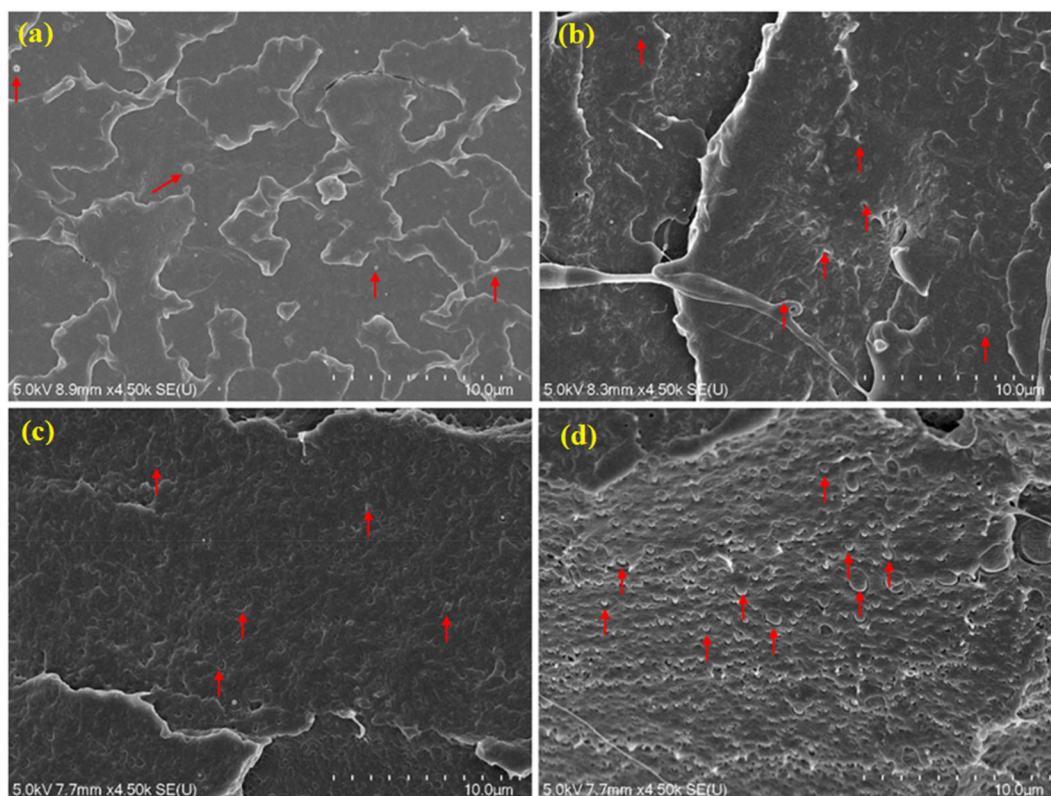


FIGURE 3 Scanning electron microscopy images of the fractured surface of PLA/PBS blends containing (a) 5 (b) 10 (c) 15, and (d) 20 wt.% PBS after tensile testing. PBS, polybutylene succinate; PLA, poly(lactic acid). [Color figure can be viewed at wileyonlinelibrary.com]

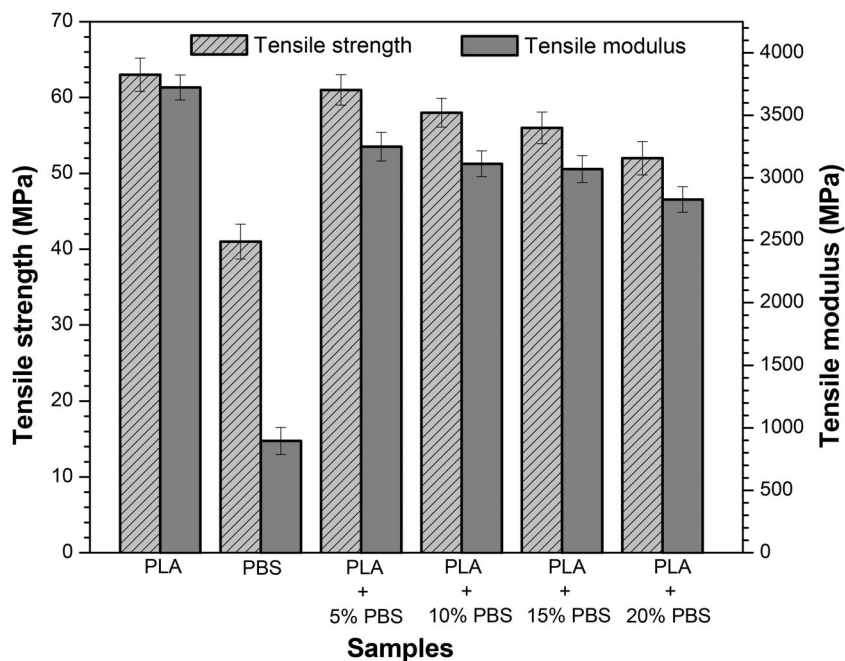


FIGURE 4 Tensile strength and tensile modulus of PLA, PBS, and PLA/PBS blends containing different wt.% PBS. PBS, polybutylene succinate; PLA, poly(lactic acid).

incorporation of PBS in the PLA matrix resulted in a decrease in the TS and TM. These decreases became larger as the PBS content increased from 5 to 20 wt.% such that compared to PLA, the largest reductions in TS

an TM were observed for the PLA-PBS blend with the highest PBS content (20 wt.%). This is not unexpected, considering the lower TS and TM of PBS as illustrated in Figure 4. Besides the low mechanical properties of PBS,

FIGURE 5 Tensile strength and tensile modulus of PLA, PLA/PBS blend, harakeke fiber-reinforced PLA/PBS composite, and harakeke fiber-reinforced PLA/PBS DCP composite with DCP. DCP, dicumyl peroxide; PBS, polybutylene succinate; PLA, poly(lactic acid).

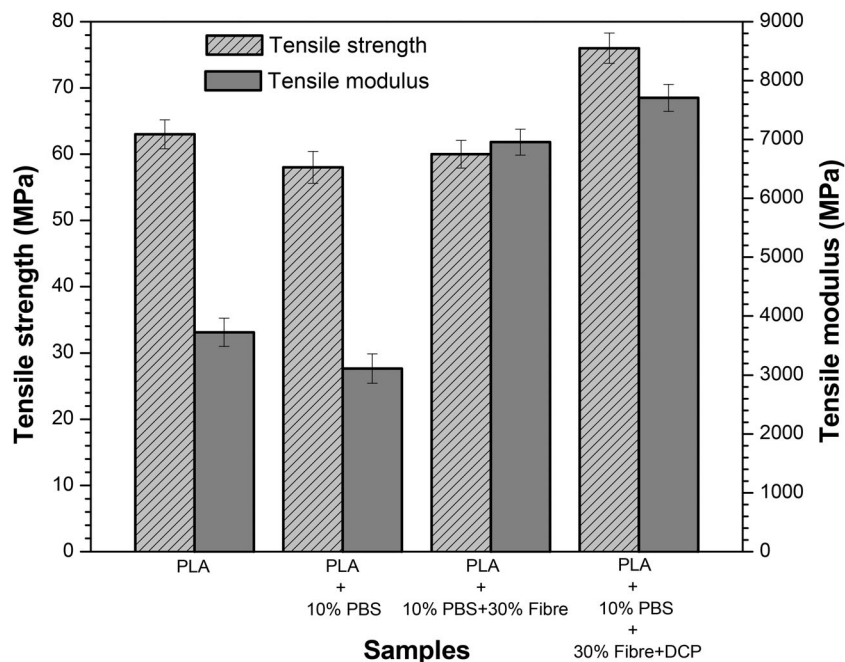


TABLE 3 Mechanical properties of PLA, PBS, PLA/PBS blend, reinforced PLA/PBS composite, and PLA/PBS composite with DCP.

| Sample code | Tensile strength (MPa) | Tensile modulus (MPa) | Elongation @ break (%) |
|--------------------------------|------------------------|-----------------------|------------------------|
| PLA | 63 | 3721 | 2.21 |
| PBS ^a | 41 | 896 | >13.51 ^a |
| PLA + 10% PBS | 58 | 3112 | 3.62 |
| PLA + 10% PBS + 30% fiber | 60 | 6955 | 2.19 |
| PLA + 10%PBS + 30% fiber + DCP | 76 | 7707 | 1.93 |

^aNeat PBS did not fracture during tensile bending. The elongation at break value recorded is the maximum value when the extensometer has reached its limit. Abbreviations: DCP, dicumyl peroxide; PBS, polybutylene succinate; PLA, poly(lactic acid).

the SEM images in Figure 3 show that PBS and PLA are only partially miscible, similar to reports in literature.^{16,32} Therefore, the low TS and TM of PBS, and the poor miscibility of PLA and PBS are believed to have contributed to the gradual drop in the tensile properties of the PLA-PBS blends with increasing PBS content.

Based on the tensile properties of the blends and for easy comparison, a fixed amount (10 wt.%) of PBS content was selected and used in reinforced PLA/PBS blends. Preliminary studies and previous studies have shown that the addition of 20–30 wt.% harakeke fiber in PLA produced remarkable improvement in the tensile properties of the resulting composite.^{37,38} It was reported that the alkali solution used for digestion helped to disrupt the bonding structure in harakeke fiber, eliminate binding material such as pectin, and reduced the lignin and hemicellulose content of the fiber. The SEM image of the digested fiber in Figure S1 revealed a rougher surface than the raw fiber and it also has opened pores which were reported to support mechanical interlocking

between matrices and fillers during composite production.³⁸ So, harakeke fiber (30 wt.%) was used as the reinforcement in the PLA/PBS blends. In addition, the compatibilization ability of DCP in PLA/PBS blends were reported previously.^{16,32} Therefore, DCP was incorporated in the reinforced PLA-PBS-fiber system produced, to facilitate reactive compatibilization of the components.

The tensile properties of PLA, PLA/PBS blend containing 10 wt.% PBS, reinforced PLA/PBS composite, and reinforced PLA/PBS composites with DCP are illustrated in Figure 5, while the values are presented in Table 3. As seen in Table 3, incorporation of 30 wt.% harakeke fiber in PLA produced little increase in the TS of the blend. This can be attributed to the reinforcing ability of the harakeke fiber which gave room for stress transfer within the composite. The effect of harakeke fiber inclusion is more pronounced in the TM than the TS. This is also associated with the high modulus of harakeke fiber, as reported in literature.^{37,38}

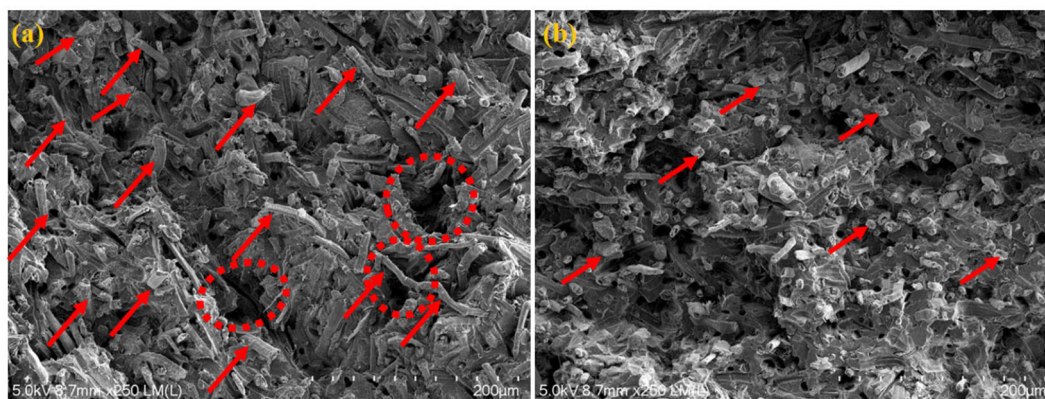


FIGURE 6 Scanning electron microscope images of the fractured surface of PLA/PBS/fiber composites (a) without DCP and (b) with DCP. DCP, dicumyl peroxide; PBS, polybutylene succinate; PLA, poly(lactic acid). [Color figure can be viewed at [wileyonlinelibrary.com](https://onlinelibrary.wiley.com/doi/10.1002/app.56030)]

Although the addition of fiber helped to increase the TS of the blend, the data in Table 3 and Figure 5 show that the TS of the PLA-PBS-fiber system (60 MPa) is still lower than the TS of neat PLA (63 MPa). This suggests a disruption in the reinforcing ability of harakeke fiber, probably due to the presence of PBS, in the PLA-PBS-fiber system. In addition, it can be due to the decrease in the actual volume of the stiffer load bearing phase (PLA) (see Table 1) within the system,⁴⁰ or the incompatibility of PLA and PBS.

Incorporation of DCP in the PLA/PBS blend helped to improve the TM of the blend but produced only marginal improvement in the TS. The TS and TM of the PLA/PBS/DCP system is lower than those of neat PLA as seen in Figure S2. In contrast, the addition of DCP helped to improve the TS and TM of the PLA-PBS-fiber system. Compared with neat PLA, the TS and TM of the DCP compatibilized harakeke-reinforced PLA/PBS blend increased by 21% and 107%, respectively. Likewise, compared with the PLA/PBS blend, incorporation of DCP increased the TS and TM of the composite with DCP by 31% and 148%, respectively. It is believed that some cross-linked/branched structures were formed during reactive blending/compounding because of the addition of DCP. Generally, the thermal decomposition of organic peroxide produces free radicals. This free radical can extract hydrogen atoms from PLA, PBS, or the fiber to generate free radicals on their main chains. This will invariably facilitate homogeneous and/or heterogeneous radical coupling reactions in form of PLA-PLA, PLA-PBS, PLA-fiber, PBS-PBS, PBS-fiber, and PLA-fiber-PBS linkages. A detailed description of the reactive compatibilization of PLA and PBS in the presence of DCP is available in literature.³² Therefore, the improved TM and TS of the composite with DCP as illustrated in Figure 5 and presented in Table 3 can be attributed to the addition of DCP, which helped to facilitate good interfacial interactions

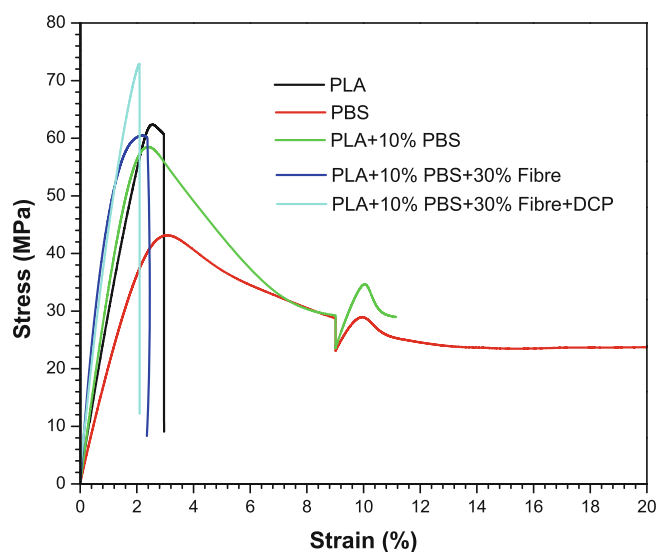


FIGURE 7 Stress-strain curves of PLA, PBS, PLA/PBS blend, reinforced PLA/PBS composite, and PLA/PBS composite with DCP. DCP, dicumyl peroxide; PBS, polybutylene succinate; PLA, poly(lactic acid). [Color figure can be viewed at [wileyonlinelibrary.com](https://onlinelibrary.wiley.com/terms-and-conditions)]

that enhanced the reinforcing ability of the fiber, compared with the composite without DCP.

The SEM images of the fractured surface (after tensile testing) of the PLA/PBS/fiber composites with and without DCP are presented in Figure 6. Figure 6a is the fractured surface of the composite without DCP while Figure 6b is the fractured surface of the composite with DCP. As seen in the figure, there are several pulled out fibers in Figure 6a, and large voids attributed to poor miscibility can also be seen in Figure 6a. This is attributed to poor interfacial interactions within the composite. In contrast, there are more of fractured fibers than pulled out fibers in Figure 6b. Fractured fibers and shorter pull-out fibers in Figure 6b indicate stronger interfacial

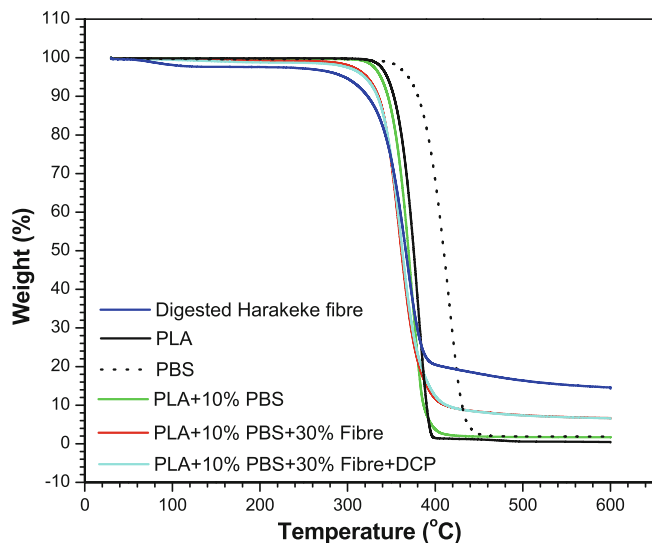


FIGURE 8 Thermogravimetric analysis curves of digested harakeke fiber, PLA, PBS, harakeke fiber-reinforced PLA/PBS composite, and harakeke fiber-reinforced PLA/PBS composite with DCP. DCP, dicumyl peroxide; PBS, polybutylene succinate; PLA, poly(lactic acid). [Color figure can be viewed at [wileyonlinelibrary.com](https://onlinelibrary.wiley.com/doi/10.1002/app.56030)]

adhesion between fiber and the matrix. This is believed to have contributed to the higher TS and TM of the composites with DCP, as discussed in the previous paragraph and shown in Figure 5 and Table 3.

To assess the effect of chain lubrication and reactive compatibilization on the toughness of the different composite systems, the elongation at break was recorded during tensile testing. The elongation at break of PLA, PBS, PLA/PBS blend containing 10 wt.% PBS, reinforced PLA/PBS composite, and reinforced PLA/PBS composite with DCP is included in Table 3 while their stress-strain curves are shown in Figure 7. As stated in Section 2.2.3, the neat PBS did not fracture during tensile testing. So, the value of elongation at break recorded for neat PBS in Table 3 is the maximum value when the extensometer reached its limit. As seen in Table 3, the elongation at break of PBS would be more than 511% higher than PLA. As for the PLA/PBS blend, the elongation at break (3.62%) is about 64% higher than neat PLA. This is not unexpected considering the higher elongation at break of PBS. However, it is significant that the addition of harakeke fiber resulted in lower elongation at break, compared with PLA and the PLA/PBS blend. This is believed to be due to the presence of harakeke fiber, restricting the effective lubrication activities of PBS on the PLA chains. More surprising is the further reduction in the elongation at break of the composite with DCP (1.93%) compared with all the other samples. Whereas reactive compatibilization using DCP helped to improve the TS

and TM of reinforced PLA/PBS blend, its elongation at break and most probably toughness decreased.

3.3 | Thermogravimetric analysis

The TGA curves of digested harakeke fiber, PLA, PBS, PLA/PBS blend containing 10 wt.% PBS, reinforced PLA/PBS composite, and reinforced PLA/PBS composite with DCP are illustrated in Figure 8. The onset temperature for thermal degradation of the materials (T_{onset}), and their thermal degradation temperatures (T_d) are summarized in Table 4. It is evident in Figure 8 and Table 4 that PBS is more thermally stable than PLA. This supports that it can be used at higher temperatures compared with PLA. Figure 8 and Table 4 also show that the thermal stability of PLA is higher than the PLA/PBS blend, and the composites. As discussed in Sections 3.1, 3.2, and shown in Figure 3, PLA and PBS are incompatible and poorly miscible; based on this the voids created by the poor miscibility can serve as heat ingress sites which would permit excessive penetration of heat into the samples, thereby lowering its thermal stability. This might be responsible for the lower observed thermal stability of the PLA/PBS blend, compared with neat PLA. Similarly, it was stated in Section 3.2 that the lower TS of the reinforced PLA-PBS composites might have resulted from PBS molecules which are poorly miscible with PLA, thereby affecting effectiveness of the reinforcing filler. This might have contributed to the reduced thermal stability of the reinforced PLA-PBS composite, compared with neat PLA. In addition, the lower thermal stability of the reinforced PLA-PBS composite can be attributed to the lower thermal stability of harakeke fiber, compared with the PLA,³⁸ and PBS. As seen in Figure 8 and Table 4, the onset temperature of thermal degradation is lower in the fiber compared with PLA and PBS, with the fiber showing an initial weight loss around 90–130°C which is due to the evaporation of preabsorbed moisture. This is believed to have contributed to the lower thermal stability of the reinforced composites.

The incorporation of DCP helped to slightly raise the thermal degradation temperature of the PLA-PBS-fiber system. This can be attributed to the reactive compatibilization properties of DCP, which might have helped to facilitate improved interfacial interactions within the system, thereby slowing down heat penetration. Generally, there is the possibility for the creation of heat ingress sites in composites. Therefore, the high thermal stability of PBS, coupled with the improved interfacial adhesion believed to have been facilitated by the inclusion of DCP (Section 3.2), might have helped to slightly improve the thermal stability of the composites with DCP (Table 4).

TABLE 4 TGA and DSC parameters of digested harakeke fiber, PLA, PBS, harakeke fiber-reinforced PLA/PBS composite, and harakeke fiber reinforced PLA/PBS composite with DCP.

| Samples | TGA | | DSC | | | |
|---------------------------------|---|---------------------------------------|---------------------------------------|---------------------------------------|---------------------------------------|----------------------|
| | T_{onset} ($^{\circ}\text{C}$) | T_{d} ($^{\circ}\text{C}$) | T_{g} ($^{\circ}\text{C}$) | T_{c} ($^{\circ}\text{C}$) | T_{m} ($^{\circ}\text{C}$) | I_{DCs} (%) |
| Fiber | 296 | 367 | - | - | - | - |
| PLA | 345 | 375 | 64.58 | 129.52 | 153.68 | 11.05 |
| PBS | 369 | 409 | - | - | 117.23 | - |
| PLA + 10% PBS | 338 | 370 | 63.62 | 115.68 | 149.75 | 29.56 |
| PLA + 10% PBS + 30% fiber | 322 | 361 | 65.84 | 116.83 | 151.87 | 35.02 |
| PLA + 10% PBS + 30% fiber + DCP | 319 | 362 | 64.93 | 119.17 | 151.89 | 33.34 |

Abbreviations: DCP, dicumyl peroxide; DSC, differential scanning calorimetry analysis; PBS, polybutylene succinate; PLA, poly(lactic acid); TGA, thermogravimetric analysis.

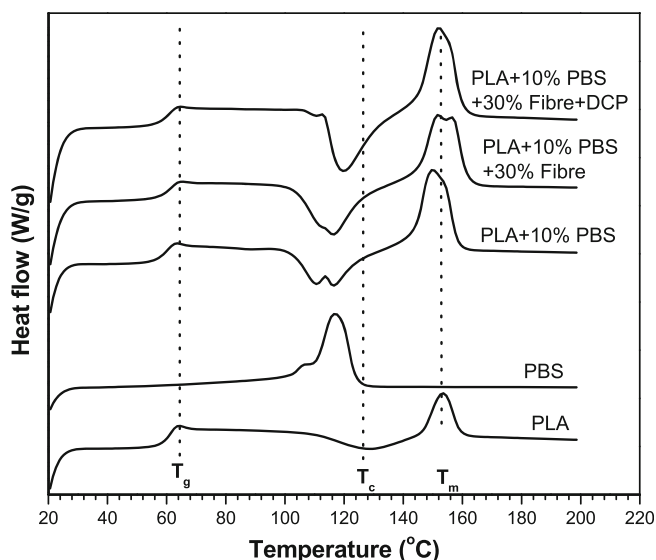


FIGURE 9 Differential scanning calorimetry analysis curves of PLA, PBS, PLA/PBS blend, harakeke fiber-reinforced PLA/PBS composite, and harakeke fiber-reinforced PLA/PBS composite with DCP. DCP, dicumyl peroxide; PBS, polybutylene succinate; PLA, poly(lactic acid).

3.4 | Differential scanning calorimetric analysis

The DSC curves of PLA, PBS, PLA/PBS blend containing 10 wt.% PBS, reinforced PLA/PBS composite, and reinforced PLA/PBS composite with DCP are illustrated in Figure 9, while the DSC data are included in Table 4. As seen in Figure 9, the glass transition (T_{g}) peak is not noticeable in the DSC curve of neat PBS, due to the low T_{g} of PBS (-40°C) which is outside the temperature range used for the samples. Likewise, PBS did not show any distinct crystallization (T_{c}) peak, the only noticeable peak being the melting point peak around 117°C .

Table 4 shows that the T_{g} of the PLA/PBS blend is slightly lower than the T_{g} of neat PLA. This is attributed

to the poor miscibility of PLA and PBS as discussed in Section 3.1 and as stated in Section 3.3, which might have disrupted the molecular bonds in PLA chains, thereby allowing the chains to move more easily. Incorporation of harakeke fiber helped to slightly improve the T_{g} of PLA, while also shifting the T_{c} to a lower temperature region. This suggests that the fiber helped to restrict the mobility of the PLA chains, while also acting as nucleating agents for crystal formation and crystal growth. This is supported by the higher CrI% of the reinforced composites (Table 4), and it aligns with what has been previously reported in literature.⁴¹

Generally, the inherent bulk crystallinity of semicrystalline materials like PLA often helps to enhance their mechanical properties.⁴² Therefore, the improved crystallization activity of PLA in the reinforced composites brought about by nucleation of PLA on the PBS molecules and the fiber are likely to have contributed to the increase in TS and TM of the reinforced composites as illustrated in Figure 5 and discussed in Section 3.2.

3.5 | Dynamic mechanical analysis

The thermomechanical properties of PLA, PLA/PBS blend, reinforced PLA/PBS composite, and reinforced PLA/PBS composite with DCP are illustrated through the DMA presented in Figure 10. It should be noted that the storage modulus (E') and tan delta values of neat PBS are not included in the figure because of the temperature range selected for this analysis. The variation in storage modulus (E') of the samples with temperature is presented in Figure 10a. There are no significant changes in the E' of the samples below the glass transition region of PLA, but the E' falls sharply around this region. In addition, it is evident from Figure 10a, that the E' of the neat PLA is higher than the PLA/PBS blend, but lower than the reinforced PLA-PBS system and reinforced PLA-PBS

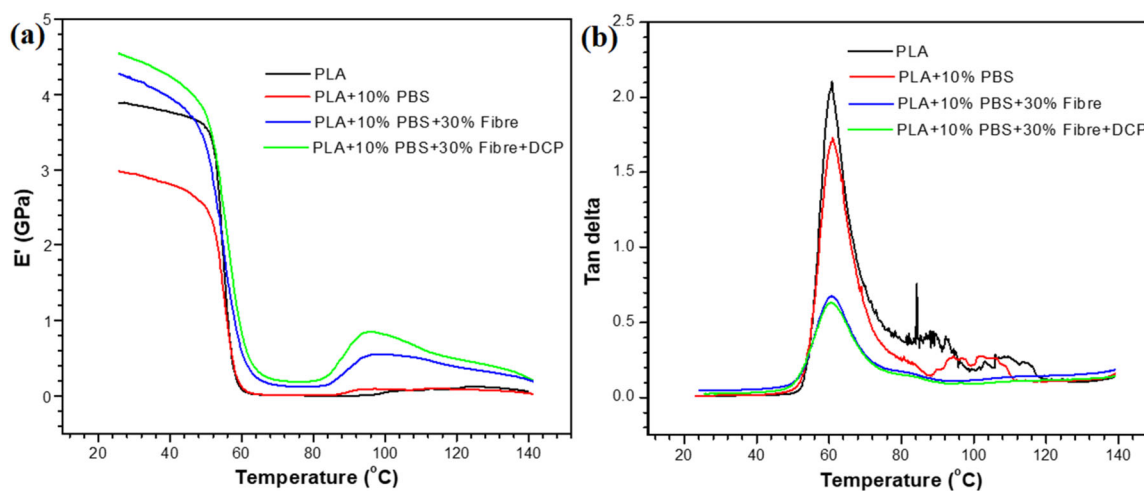


FIGURE 10 Thermomechanical properties of PLA, PLA/PBS blend, harakeke fiber-reinforced PLA/PBS composite, and harakeke fiber-reinforced PLA/PBS composite with DCP. DCP, dicumyl peroxide; PBS, polybutylene succinate; PLA, poly(lactic acid). [Color figure can be viewed at [wileyonlinelibrary.com](https://onlinelibrary.wiley.com/doi/10.1002/app.56030)]

composite with DCP. This aligns with the mechanical test results discussed in Section 3.2.

Different factors can contribute to the E' of polymer blends and composites including matrix type, filler type, dispersion of filler, and interfacial adhesion.^{36,43} Therefore, the higher E' of the composites is attributed to the presence of harakeke fiber in the composites, which due to its high stiffness, can impose some stiffness on PLA, thereby facilitating interfacial stress transfer within the composites. This also supports the good reinforcing ability of harakeke fiber as reported in literature.^{37,38} In addition, it is noteworthy that whereas the incorporation of harakeke produced remarkable improvement in the E' of the PLA/PBS blend, the addition of both harakeke fiber and DCP produced further increase in the E' such that the E' of the composite with DCP is higher than that of the composite without DCP. This is believed to be due to the reactive compatibilization of PLA with PBS as reported in literature,^{16,32} and possibly the coupling activity of DCP on components of the PLA-PBS-fiber-DCP system thereby aligning with the mechanical test result presented in Figure 5 and discussed in Section 3.2. Coupling activities at the interface of the components would help to improve adhesion, and this might have enhanced the ability of PLA in the composites to withstand larger mechanical constraints through recoverable viscoelastic deformation.

The interfacial adhesion within the systems was further investigated from the loss factor or damping parameter ($\tan \delta$) of the samples. The $\tan \delta$ of composites is largely influenced by the concentration of shear stress and viscoelastic energy dissipation,⁴⁴ thereby causing the $\tan \delta$ to depend largely on the interfacial adhesion

between the filler and the matrix. Generally, lower $\tan \delta$ values are obtained when the interfacial adhesion is high while a weak adhesion will result in higher $\tan \delta$ values.⁴⁴ The $\tan \delta$ plot of PLA, PLA/PBS blend containing 10 wt.% PBS, harakeke fiber-reinforced PLA/PBS composite, and harakeke fiber-reinforced PLA/PBS composite with DCP is illustrated in Figure 10b. As seen in Figure 10b, the $\tan \delta$ value of PLA is significantly higher than the composites. This can be attributed to the reduced volume of matrix in the composites and restriction of PLA chain mobility by the fiber. In addition, the lower $\tan \delta$ peak of the composites indicates higher load bearing capacity of the composites, attributed to the adhesion of the fiber to the PLA matrix and effective stress transfer within the composite. Compared with the composites, the $\tan \delta$ peak of the PLA/PBS blend is higher. This indicates poor adhesion between PLA and PBS and is attributed to the poor miscibility of PLA and PBS (Figure 3) and as such confirms the incompatibility of PLA and PBS as discussed in previous sections. However, compared to neat PLA, the low $\tan \delta$ of the PLA/PBS blends suggests that there is some degree of interaction between PLA and PBS.

4 | CONCLUSIONS

Concurrent compatibilization and reinforcement of PLA/PBS blend were achieved. Incorporation of varying amounts of PBS in PLA to produce PLA/PBS blends resulted in reduced mechanical performance of the resulting blends due to incompatibility and poor miscibility of PLA and PBS as seen through SEM investigations.

Addition of harakeke fiber as reinforcement in the PLA/PBS blends was not enough to raise the TS of the resulting PLA-PBS composite to values above that of neat PLA. This is attributed to possible reduction in the effectiveness of harakeke fiber to reinforce the PLA/PBS blend, due to the poorly miscibility of PBS and PLA. Simultaneous reactive compatibilization and reinforcement of the PLA/PBS blends produced significant increases in the TS, TM, storage modulus, and crystallinity of the resulting composite. Regarding the elongation at break, the incorporation of harakeke seemed to have restricted the effective lubrication activities of PBS on the PLA chains. Whereas reactive compatibilization using DCP helped to improve the TS and TM of reinforced PLA/PBS blend, it does not seem to have had any positive impact on the toughness or elongation at break of the resulting composite. Overall, the main outcome of this study shows that PLA/PBS can be reactively compatibilized and reinforced at the same time thereby leading to the production of composites with significantly higher mechanical, thermal, and thermomechanical performance. Nevertheless, further research is recommended for exploring other compatibilizers that are more suitable for reinforced PLA/PBS blends to produce effectively reinforced, and toughened blends suitable for more diverse structural applications.

AUTHOR CONTRIBUTIONS

John O. Akindoyo: Conceptualization (lead); formal analysis (lead); investigation (lead); methodology (lead); writing — original draft (lead); writing — review and editing (lead). **Kim Pickering:** Funding acquisition (lead); supervision (lead). **Mohammad Dalour Beg:** Supervision (supporting); writing — review and editing (supporting). **Michael Mucalo:** Supervision (supporting); writing — review and editing (supporting).

ACKNOWLEDGMENTS

The authors acknowledge the funding from the New Zealand Ministry of Business, Innovation and Employment, under the Āmiomio Aotearoa project hosted by The University of Waikato (UOWX2004). The first author also appreciates the financial support through a Research & Enterprise Award (108023) provided by the University of Waikato. Open access publishing facilitated by The University of Waikato, as part of the Wiley - The University of Waikato agreement via the Council of Australian University Librarians.

DATA AVAILABILITY STATEMENT

The data that support the findings of this study are available from the corresponding author upon reasonable request.

ORCID

John O. Akindoyo  <https://orcid.org/0000-0002-7701-123X>

REFERENCES

- [1] Z. Gu, J. Zhang, W. Cao, X. Liu, J. Wang, X. Zhang, W. Chen, J. Bao, *Polymer* **2022**, *262*, 125454.
- [2] S. M. Rangappa, S. Siengchin, H. N. Dhakal, *Appl. Sci. Eng. Prog.* **2020**, *13*, 183.
- [3] Y. G. Thyavihalli Girijappa, S. Mavinkere Rangappa, J. Parameswaranpillai, S. Siengchin, *Front. Mater.* **2019**, *6*, 226.
- [4] R. Arrigo, A. D'Anna, A. Frache, *Mater. Today Sustain.* **2023**, *21*, 100314.
- [5] I. Wojnowska-Baryła, D. Kulikowska, K. Bernat, *Sustainability* **2020**, *12*, 2088.
- [6] X. Chen, N. Yan, *Mater. Today Sustain.* **2020**, *7*, 100031.
- [7] A. Bartos, K. Nagy, J. Anggono, H. Purwaningsih, J. Móczó, B. Pukánszky, *Compos. A: Appl. Sci. Manuf.* **2021**, *143*, 106273.
- [8] A. Mtibe, M. P. Motloung, J. Bandyopadhyay, S. S. Ray, *Macromol. Rapid Commun.* **2021**, *42*, 2100130.
- [9] K. Hu, D. Huang, H. Jiang, S. Sun, Z. Ma, K. Zhang, L. Pan, Y. Li, *ACS Omega.* **2019**, *4*, 19777.
- [10] K. Hamad, M. Kaseem, H. Yang, F. Deri, Y. Ko, *Express Polym Lett.* **2015**, *9*, 435.
- [11] A. D'Anna, R. Arrigo, A. Frache, *J. Polym. Environ.* **2022**, *30*, 102.
- [12] N. Tripathi, M. Misra, A. K. Mohanty, *ACS Eng. Au.* **2021**, *1*, 7.
- [13] R. M. Rasal, A. V. Janorkar, D. E. Hirt, *Prog. Polym. Sci.* **2010**, *35*, 338.
- [14] R. Banerjee, S. S. Ray, *Polym. Eng. Sci.* **2021**, *61*, 617.
- [15] A. Ahmad, F. Banat, H. Alsafar, S. W. Hasan, *Biomass Convers. Biorefin.* **2022**, *14*, 1.
- [16] H. Cai, C. Cao, Y. Zheng, D. Liu, X. Xia, X. Sun, X. Liu, L. Xiao, Q. Qian, Q. Chen, *Macromol. Mater. Eng.* **2023**, *308*, 2200581.
- [17] Y. Chen, W. Wang, D. Yuan, C. Xu, L. Cao, X. Liang, *ACS Sustain. Chem. Eng.* **2018**, *6*, 6488.
- [18] P. Ma, D. Hristova-Bogaerds, J. Goossens, A. Spoelstra, Y. Zhang, P. Lemstra, *Eur. Polym. J.* **2012**, *48*, 146.
- [19] K. S. Anderson, M. A. Hillmyer, *Polym.* **2004**, *45*, 8809.
- [20] I. Fortelny, A. Ujcic, L. Fambri, M. Slouf, *Front. Mater.* **2019**, *6*, 206.
- [21] M. Mohammadi, M.-C. Heuzey, P. J. Carreau, A. Taguet, *Nanomaterials* **2021**, *11*, 857.
- [22] T. Messin, S. Marais, N. Follain, A. Guinault, V. Gaucher, N. Delpouve, C. Sollogoub, *J. Membr. Sci.* **2020**, *598*, 117777.
- [23] K. Changwichean, T. Silalertruksa, S. H. Gheewala, *Sustainability* **2018**, *10*, 952.
- [24] Y. Deng, N. L. Thomas, *Eur. Polym. J.* **2015**, *71*, 534.
- [25] E. Fortunati, D. Puglia, A. Iannoni, A. Terenzi, J. M. Kenny, L. Torre, *Materials* **2017**, *10*, 809.
- [26] R. Supthanyakul, N. Kaabuuathong, S. Chirachanchai, *Polymer* **2016**, *105*, 1.
- [27] L. Aliotta, A. Vannozi, L. Panariello, V. Gigante, M.-B. Coltelli, A. Lazzeri, *Polymer* **2020**, *12*, 1366.
- [28] N. Zhang, Q. Wang, J. Ren, L. Wang, *J. Mater. Sci.* **2009**, *44*, 250.
- [29] T. Kanzawa, K. Tokumitsu, *J. Appl. Polym. Sci.* **2011**, *121*, 2908.

- [30] M. Harada, T. Ohya, K. Iida, H. Hayashi, K. Hirano, H. Fukuda, *J. Appl. Polym. Sci.* **2007**, *106*, 1813.
- [31] G.-X. Chen, H.-S. Kim, E.-S. Kim, J.-S. Yoon, *Polymer* **2005**, *46*, 11829.
- [32] D. Ji, Z. Liu, X. Lan, F. Wu, B. Xie, M. Yang, *J. Appl. Polym. Sci.* **2014**, *131*, 39580.
- [33] S. Chuayjuljit, C. Wongwaiwattanukul, P. Chaiwutthinan, P. Prasassarakich, *Polym. Compos.* **2017**, *38*, 2841.
- [34] L. He, F. Song, D.-F. Li, X. Zhao, X.-L. Wang, Y.-Z. Wang, *ACS Sustain. Chem. Eng.* **2020**, *8*, 1573.
- [35] S. Vorawongsagul, P. Pratumpong, C. Pechyen, *Food Packag. Shelf Life.* **2021**, *27*, 100608.
- [36] J. O. Akindoyo, M. D. H. Beg, S. Ghazali, H. P. Heim, M. Feldmann, M. Mariatti, *J. Appl. Polym. Sci.* **2021**, *138*, 49752.
- [37] M. D. H. Beg, K. L. Pickering, C. Gauss, *Compos. A: Appl. Sci. Manuf.* **2023**, *166*, 107384.
- [38] J. O. Akindoyo, K. Pickering, M. D. Beg, M. Mucalo, *Compos. A: Appl. Sci. Manuf.* **2023**, *164*, 107326.
- [39] R.-y. Chen, W. Zou, C.-r. Wu, S.-k. Jia, Z. Huang, G.-z. Zhang, Z. T. Yang, J. P. Qu, *Polym. Test.* **2014**, *34*, 1.
- [40] R. M. Taib, Z. A. Ghaleb, Z. A. Mohd Ishak, *J. Appl. Polym. Sci.* **2012**, *123*, 2715.
- [41] J. O. Akindoyo, M. D. Beg, S. Ghazali, H. P. Heim, M. Feldmann, *Compos. A: Appl. Sci. Manuf.* **2017**, *103*, 96.
- [42] K. Pongtanayut, C. Thongpin, O. Santawitee, *Energy Procedia.* **2013**, *34*, 888.
- [43] J. O. Akindoyo, M. D. H. Beg, S. B. Ghazali, M. R. Islam, A. A. Mamun, *Polym.-Plast. Technol. Eng.* **2015**, *54*, 1321.
- [44] K. V. Krishna, K. Kanny, *Compos. Part B.* **2016**, *104*, 111.

SUPPORTING INFORMATION

Additional supporting information can be found online in the Supporting Information section at the end of this article.

How to cite this article: J. O. Akindoyo, K. Pickering, M. D. Beg, M. Mucalo, *J. Appl. Polym. Sci.* **2024**, *141*(40), e56030. <https://doi.org/10.1002/app.56030>